Tellus (2002), 54A, 288–298

TELLUS
ISSN 0280–6495

Interdecadal changes in the zonal wind and the intensity of intraseasonal oscillations during boreal summer Asian monsoon

By I. I. ZVERYAEV*, *International Pacific Research Center, SOEST, University of Hawaii at Manoa, Honolulu, Hawaii, USA*

(Manuscript received 1 August 2000; in final form 29 November 2001)

ABSTRACT

Decadal–interdecadal changes in the intensity of intraseasonal oscillations (ISO) and in the summer mean wind fields in the Asian monsoon system are investigated using 51 yr of 850 hPa zonal wind data obtained from the National Centers for Environmental Prediction – National Center for Atmospheric Research (NCEP/NCAR) Reanalysis. Decadal–interdecadal variations contribute significantly to the total variability of the summer mean 850 hPa zonal wind (30–45%) and the ISOs intensity (20–35%). These variations in the summer mean 850 hPa zonal wind and in the intensity of the 30–60 d ISO have a distinct zonal structure and are associated with the strength of low level westerlies and with meridional dynamics of the Tropical Convergence Zone (TCZ). Interdecadal changes in the intensity of the 10–20 d ISO are most pronounced over the eastern Indian Ocean, the South China Sea and the western tropical Pacific.

Singular value decomposition (SVD) analysis revealed a strong correlation on an interdecadal timescale between the sea surface temperatures (SST) in the Indian Ocean and the summer mean 850 hPa zonal wind and the intensity of the ISOs in the Asian summer monsoon, whereas such correlations on a decadal timescale are weak. The temporal expansion coefficients of the first SVD mode show a climate regime shift in the mid-late 1970s. During the last few decades, SST in the Indian Ocean increased, resulting in a decreased land–sea heat contrast and weaker low-level westerlies over northern Indian Ocean, the Indian subcontinent, and Indochina. In response to sea surface warming and associated enhanced convection, the 30–60 d ISO became stronger over the equatorial central and western Indian Ocean and the South China Sea, and weaker over the Indian subcontinent, the northern Arabian Sea and the Bay of Bengal. Meanwhile a 10–20 d ISO intensified over the eastern Indian Ocean, the South China Sea, and the western tropical Pacific.

1. Introduction

Intraseasonal oscillations (ISOs) represent one of the strongest signals in the Asian summer monsoon. These ISOs are characterized by active/break cycles, with dominant periods between 10–20 d and 30–60 d (Krishnamurti and Bhalme, 1976; Gadgil and Asha, 1992). It was shown that, in general, the 10–20 d oscillation propagates westward, while the 30–60 d oscillation propagates northward. Known ISO studies (Hartmann and Michelsen, 1989; Gadgil and Asha, 1992; Wang and Xu, 1997; Chen and Weng, 1999; Kang et al., 1999) have focused mostly on the origin and the climatological aspects of the ISOs.

* Current affiliation and address for correspondence: P. P. Shirshov Institute of Oceanology, RAS, 36 Nakhimovsky Avenue, Moscow, 117218, Russia.
e-mail: igorz@sail.msk.ru

The relationship between intraseasonal and interannual variability of the monsoon has been studied in several papers (Lau and Chan, 1988; Ferranti et al., 1997; Chen and Weng, 1999; Slingo et al., 1999). Chen and Weng (1999) have shown a pronounced interannual variation in the frequency of monsoon depressions in the Bay of Bengal and an enhancement (reduction) of monsoon depression activity occurring during cold (warm) summers. The observational study of Lau and Chan (1988) and model results obtained by Ferranti et al. (1997) demonstrated that the intraseasonal variability in the monsoon system was spatially correlated with the interannual variations. Later Sperber et al. (2000) identified a common mode for intraseasonal and interannual monsoon variations over India. Therefore, the intraseasonal and interannual monsoon fluctuations may have a common mode of variability. Recent results by Annamalai et al. (1999), Sperber et al. (2000) and Waliser et al. (2001), however, suggest that links between ISO activity and interannual (particularly, ENSO-related) variability of the sea surface temperature (SST) are relatively weak. Moreover, analyzing observed rainfall data over India, Krishnamurthy and Shukla (2000) found quite different spatial patterns for intraseasonal and interannual monsoon variations. This result is somewhat contradictory to the model-based results of Ferranti et al. (1997).

Monsoon variations on timescales longer than interannual have been studied little. In the recent excellent survey by Webster et al. (1998) of the current state and progress of monsoon studies, the section on interdecadal monsoon variability is the shortest one. It refers to results of Parthasarathy et al. (1994) and Shukla (1995), who found that, during the last decades, the life cycle of El Niño–Southern Oscillation (ENSO) changed, as did the relationship between El Niño and the Indian monsoon. Mehta and Lau (1997) have shown that the high coherence between the SST and rainfall anomalies at decadal–multidecadal timescales occurred between slow, 'meandering' variabilities in both quantities with no distinct decadal–multidecadal periodicities. In their recent study, Torrence and Webster (1999) demonstrated that the ENSO/monsoon variance contains an amplitude modulation on a 12–20-yr timescale. Moreover, Weng et al. (1999) found that the relationship between southwest monsoon and SST anomalies in the eastern tropical Pacific differed on decadal and interannual timescales. On the decadal timescale, the southwest summer monsoon intensified during periods of a warmer eastern tropical Pacific, whereas on the interannual timescale the monsoon usually weakened during El Niño events. These results suggest that the mechanisms linking monsoon variations to anomalous SST may be different on decadal and interannual timescales.

While decadal–interdecadal changes in the mean state of the monsoon have been recognized (though not well studied), probably the only evidence for such variations in ISOs has been presented by Slingo et al. (1999). Using data from the National Centers for Environmental Prediction–National Center for Atmospheric Research (NCEP/NCAR) Reanalysis, they detected a decadal variability in the activity of Madden–Julian oscillation (MJO) (Madden and Julian, 1971; 1972) and confirmed their results with model simulations. These results suggest that decadal variations in SST may produce changes in the MJO activity during boreal winter.

Study of decadal–interdecadal variations in the ISOs requires a relatively long (several decades at least) record with a reasonably high resolution in time and space. Recently available data from the NCEP/NCAR Reanalysis (Kalnay et al., 1996) allows such a long-term analysis. In the present study we use the relatively continuous and homogeneous data on 850 hPa zonal wind available from the NCEP/NCAR Reanalysis to analyze decadal–interdecadal variations in ISO intensity. We also study the relationship of these variations and long-term variations in the mean summer zonal wind to SST variations in the Indian Ocean. The data and methods used are described in Section 2. Climatology and general time–space structure of year-to-year variations in the ISO intensity and in the seasonal mean 850 hPa zonal wind are discussed in Section 3. In Section 4 we use singular value decomposition (SVD) analysis to examine dominant modes of decadal–interdecadal variations and links to SST changes in the Indian Ocean. Finally, concluding remarks are given in Section 5.

2. Data and methods

In our analysis we used daily and monthly 850 hPa zonal wind data from the NCEP/NCAR

Reanalysis for 1948–1998 (Kalnay et al., 1996). The NCEP/NCAR Reanalysis provides all the parameters for a 6-h temporal resolution and a 2.5° latitude by 2.5° longitude spatial resolution over a period of more than 50 yr. This allows an explicit description of short-term variability. Since the zonal wind data in NCEP/NCAR Reanalysis are classified as A data, they are based heavily on observed data and among the most reliable (Kalnay et al., 1996). Intraseasonal variability is well pronounced in the 850 hPa wind, and this variable is widely used in ISO studies (Annamalai et al., 1999; Sperber et al., 2000; Waliser et al., 2001). In this study, we also used NCEP/NCAR Reanalysis data on vertical velocity (ω) at 500 hPa for the same period. Our analysis is limited to latitudes 20°S–30°N and longitudes 40°E–130°E, a region containing the major components of the monsoon circulation.

Also, in the present study we used data from the Reconstructed Reynolds SST data provided by the NOAA-CIRES Climate Diagnostics Center, Boulder, Colorado, at http://www.cdc.noaa.gov/. To produce this data set the dominant EOF modes were used as basis functions and were fitted to the in situ data to determine the time dependence of each mode. Global fields of SST were then reconstructed from these spatial and temporal modes (Reynolds and Smith, 1994; Smith et al., 1996). In our study we used the monthly means from January 1950 through December 1997 on the 2° latitude × 2° longitude grid to form summer seasonal means for a singular value decomposition (SVD) analysis.

In our study we define ISO intensity as the standard deviations (std) of band-passed intraseasonal variability of the daily 850 hPa zonal wind over the 153 d in each summer monsoon season (May–September, hereafter MJJAS). More specifically, for each dominant ISO time scale (i.e. 30–60 and 10–20 d, hereafter referred to ISO-1 and ISO-2, respectively; Ju and Slingo, 1995; Vernekar and Ji, 1999) we performed band-pass filtering with the Lanczos filter (Lanczos, 1956; Duchon, 1979), which provides a very effective cutoff for the selected frequency band, and then computed the std of this band-passed daily data. To characterize year-to-year variability we computed the standard deviations (STD) over the 51 years of the seasonal ISO-1 and ISO-2 intensities and also over the 51 summer (MJJAS) seasonal mean zonal wind. In order to distinguish between std (day-to-day variability) and STD (year-to-year variability) we refer further in the paper to the former as ISO intensity, and to the latter as STD.

To examine the spatio-temporal structure of long-term variations of the seasonal mean zonal wind and the intensities of ISO-1 and ISO-2, we applied 5-yr running mean filter to eliminate tropospheric biennial oscillation (TBO) and interannual (ENSO related) variability. Therefore, the low-pass filtered time series represents the decadal–interdecadal component of the total variability.

To define dominant modes of decadal–interdecadal variability and ascertain their relationship to SST variations in the Indian Ocean, we performed singular value decomposition (SVD) of the covariance matrix between each field of the three monsoon variables (i.e 850 hPa seasonal mean zonal wind, ISO-1 and ISO-2 intensities) and the Indian Ocean SST fields. Detailed descriptions of SVD analysis can be found in Bretherton et al. (1992) and von Storch and Navarra (1995). Empirical orthogonal functions (EOF) analysis based on covariance matrix (Wilks, 1995) was applied to define dominant modes of variability of the low-pass filtered seasonal (MJJAS) mean ω.

3. Climatology and variability of the summer mean zonal wind and the intensity of ISO

The pattern of the climatological summer mean 850 hPa zonal wind (Fig. 1a) demonstrates the strong westerly flow north of the equator over the Arabian sea, the Indian subcontinent, the Bay of Bengal and Indochina. Maximum (up to 12 m s^{-1}) wind strength is observed over the Arabian Sea. During boreal spring the westerly flow develops in response to the increase of land–sea heat contrast. Later, during summer monsoon season, diabatic heating from convection maintains the monsoon circulation (Rao et al., 1989; Annamalai et al., 1999). The strong low-level westerlies are the most important component of the Asian summer monsoon. South of the equator intensive easterly flow dominates the Indian Ocean (Fig. 1a).

STD of time series of the summer mean 850 hPa zonal wind is a measure of its year-to-year variability (Fig. 1b). This variability is large along the

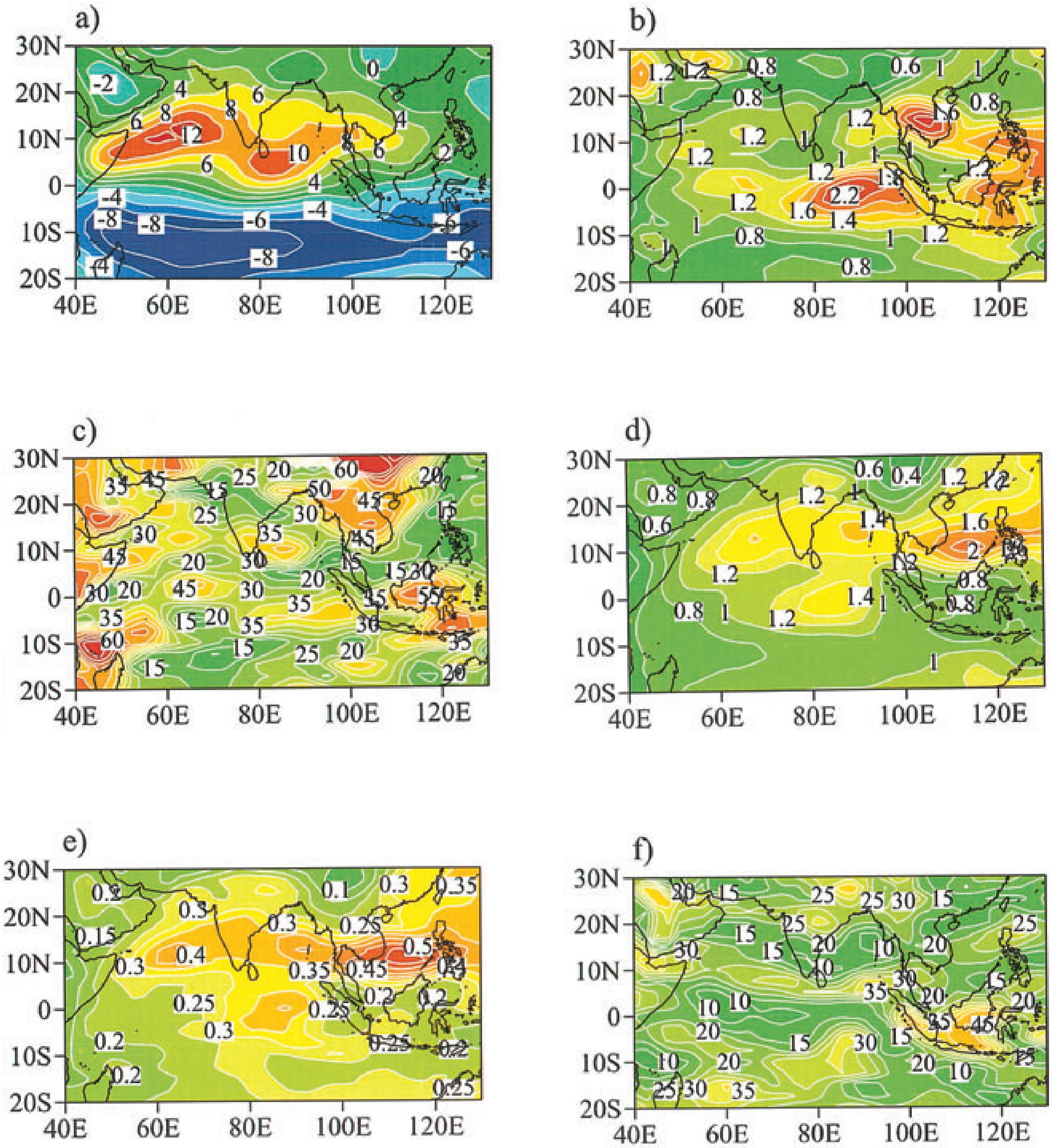

westerly flow, especially over the Arabian Sea, the Bay of Bengal and Indochina. The maximum of STD at the equator in the eastern Indian Ocean presumably does not reflect changes in wind strength, rather meridional dynamics (i.e. shifts) of zonal flow. Variability in zonal wind over the Maritime continent is of less interest because zonal wind in this region is essentially weaker (Fig. 1a).

To highlight decadal–interdecadal variations we computed STD of the low-pass filtered time series of the summer mean 850 hPa zonal wind. The spatial pattern of decadal–interdecadal variations (not shown) is, basically, the same as that of STD estimated from the unfiltered data (Fig. 1b). Estimated ratios (Fig. 1c) between variances of the low-pass filtered and unfiltered time series reflect the contribution of the decadal–interdecadal variations to the total variability of summer mean

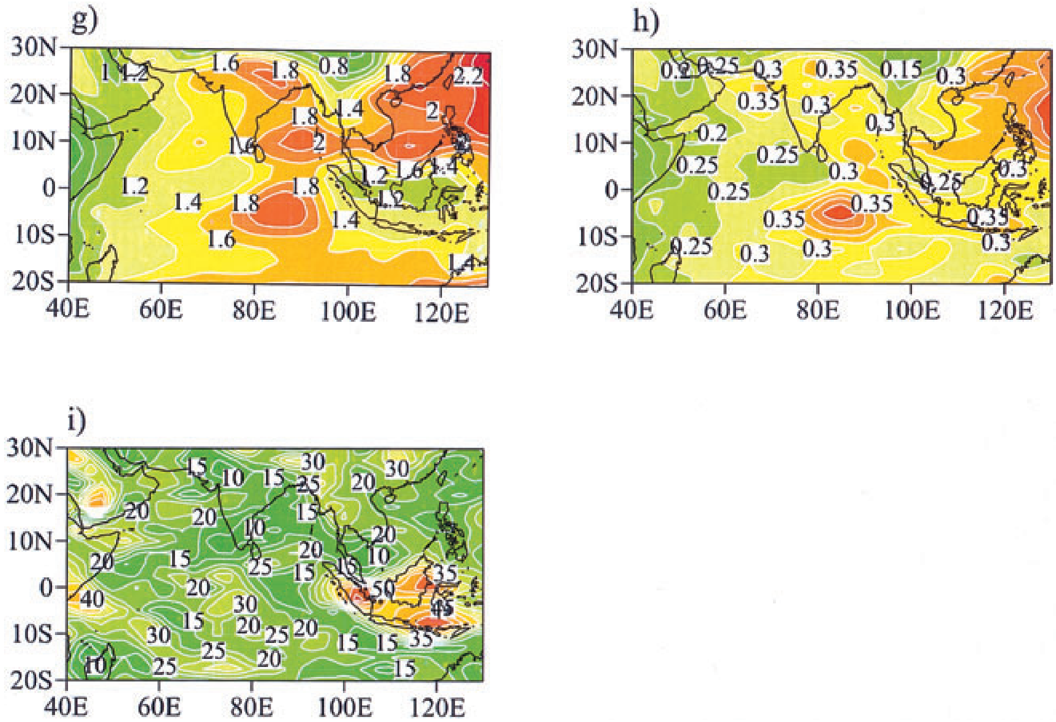

Fig. 1. Seasonal (MJJAS) mean climatologies (a, d, g), year-to-year STD's (b, e, h) and ratios (in %) between variances of low-pass filtered and unfiltered time series (c, f, i) of the 850 hPa zonal wind (a, b, c), and intensities of ISO-1 (d, e, f) and ISO-2 (g, h, i).

850 hPa zonal wind. As seen (Fig. 1c), decadal–interdecadal variations contribute significantly (30–55%) to the total variability of westerlies. In particular, the highest (45–55%) contribution to the total variability of the mean summer zonal wind is found over Indochina.

The climatology of the summer (MJJAS) intensity of ISO-1 is presented in Fig. 1d. The largest ISO-1 intensities exceeding 1.4 m s^{-1} are found along the westerly flow belt over the Arabian Sea, Indian subcontinent, the Bay of Bengal, Indochina, and the South China Sea (Fig. 1d). A secondary maximum of the ISO-1 intensity is located at the equator in the eastern Indian Ocean. We note that magnitudes of ISO-1 are higher, in general, than those of year-to-year variations of the zonal wind (Fig. 1b).

The spatial structure of the total variability of the ISO-1 intensity, presented by the STD of the unfiltered time series (i.e. original, not low-pass filtered time series of std of ISO-1), is shown in Fig. 1e. Basically, the distribution of maxima and minima is the same as that of climatology of ISO-1 (Fig. 1d). The highest variability in the intensity of ISO-1 is observed along the belt of strong westerlies (Fig. 1e). The ratio (Fig. 1f) between variances of low-pass filtered and unfiltered time series suggests that decadal scale variations play an important role in the total variability in the intensity of ISO-1. In particular, the contribution of decadal–interdecadal variations to total variability of the ISO-1 intensity is highest (up to 30–35%) over India and the Indian Ocean along 10°N and 10°S (Fig. 1f). Remarkably, locations of these maxima of contribution coincide with continental and oceanic locations of the Tropical Convergence Zone (TCZ). As was earlier shown, ISOs represent fluctuations of the TCZ between the two locations (Sikka and Gadgil, 1980; Goswami, 1994). These fluctuations are characterized by repeated TCZ propagation from the southern to the northern position during the summer monsoon season (Sperber et al., 2000; Annamalai and Slingo, 2001; Goswami and Mohan, 2001).

Major features of the climatology of the ISO-2 intensity (Fig. 1g) are principally different from those of the climatology of the ISO-1 intensity (Fig. 1d) and reflect the different genesis of ISO-2. The highest values of the ISO-2 intensity are observed over the eastern Indian Ocean from the equator to the Indian subcontinent (2 m s^{-1}) and over the western tropical Pacific (2.4 m s^{-1}) (Fig. 1g). Patterns of total year-to-year variability (Fig. 1h) and decadal–interdecadal variations (not shown) of ISO-2 intensity are similar to its climatology (Fig. 1g) and demonstrate the highest variability in the regions of high activity of ISO-2. Though decadal–interdecadal variations contribute a considerable portion to the total variability of the ISO-2 intensity (Fig. 1i), this contribution is somewhat lower than in the case of ISO-1 (Fig. 1f).

It is important to note that there is a certain similarity (though not in details) between patterns obtained for mean 850 hPa zonal (Figs. 1a and b) wind and ISO-1 (Figs. 1d and e), which suggests their close relationship. Spatial structure of climatology and variability of the ISO-2 intensity is completely different.

4. Interdecadal changes of the summer mean zonal wind and ISO intensity and their links to SST variations

To define dominant modes of decadal–interdecadal variability of the summer mean 850 hPa zonal wind and the ISO intensities and investigate their links to SST variations, we performed conventional SVD analysis (Bretherton et al., 1992) on the low-pass filtered data. Linear coupled dominant modes between fields of each of the monsoon variables (i.e. seasonal mean zonal wind, ISO-1 and ISO-2 intensities) and SST fields in the Indian Ocean were defined. It appears that the first SVD mode explains 81–86% of the total covariance, whereas each of the subsequent modes explains less than 12%. Therefore, we limit our analysis to consideration of the first SVD mode only.

The first SVD mode (SVD-1) between the low-pass filtered summer mean 850 hPa zonal wind and SST fields explains 81.9% of the total covariance. This mode explains 33.1% of the low-level zonal wind variance. The SVD-1 spatial pattern for the summer mean zonal wind (Fig. 2a) is characterized by the weakening of westerlies over the extensive region from the Arabian Sea to the South China Sea. Opposite changes in zonal wind are evident south of the equator. The SVD-1 spatial pattern for SST (Fig. 2d) shows a basin-wide SST increase in the Indian Ocean, specifically strong along the equator with maximum warming in the central and western Indian Ocean. Time series of expansion coefficients of both 850 hPa zonal wind and SST patterns (Fig. 2g) demonstrate interdecadal variations, with a prominent regime shift from positive to negative values in the mid-late 1970s. In general, the obtained patterns are consistent with results presented by Weng et al. (1999). The first SVD mode demonstrates warming of SST in the Indian ocean during the last few decades, which results, as indicated by Sperber et al. (2000), in decrease of the land–sea heat contrast in this region. In response to the decrease of heat gradient, the strength of westerlies also decreased.

The SVD-1 mode explains 82.5% of the total covariance between the low-pass filtered ISO-1 intensity and SST fields. The first mode accounts for 32.1% of the ISO-1 variance. The SVD-1 spatial pattern for the ISO-1 intensity (Fig. 2b) has an evident zonal structure north of the equator. It is characterized by the decrease of the ISO-1 intensity over the northern Arabian Sea, Indian subcontinent, and the northern Bay of Bengal, whereas south of this region, over the Indian Ocean and the South China Sea, ISO-1 became more intensive (Fig. 2b). Being different in details, the SVD-1 spatial pattern for SST (Fig. 2e) is similar in general to that presented in Fig. 2d; thus, we omit the description of its spatial structure here. As in the case of the summer mean zonal wind–SST coupled mode (Fig. 2g), the time series of expansion coefficients of both the ISO-1 intensity and SST patterns (Fig. 2h) demonstrate interdecadal variations with a prominent regime shift in the mid 1970s. These results suggest that SST warming on an interdecadal timescale caused an increase of convective activity over the Indian Ocean (specifically strong in the equatorial region) and intensification of ISO-1, whereas over the Indian subcontinent the intensity of ISO-1

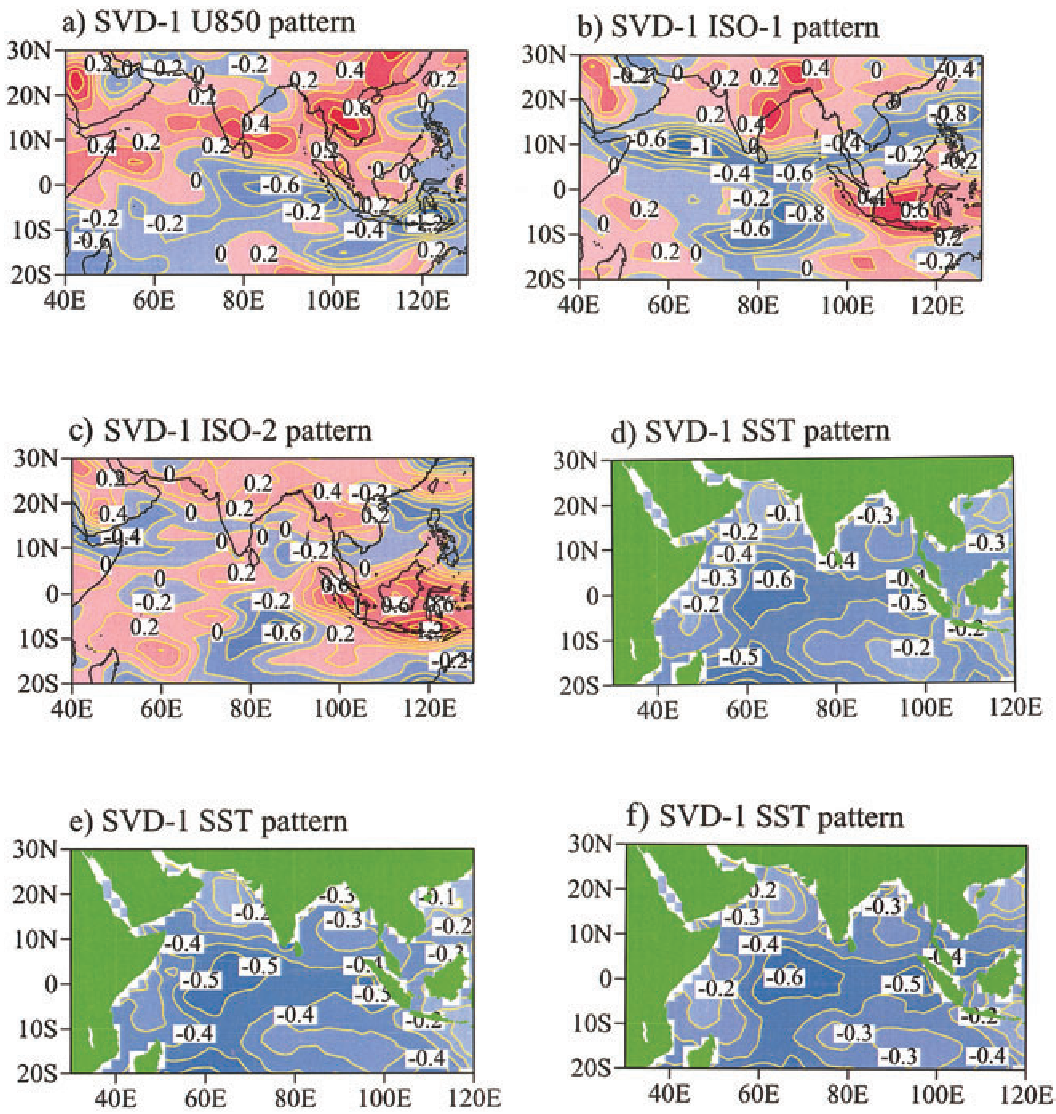

weakened. Consistent with the above results, interdecadal changes of the vertical velocity (ω) at 500 hPa, presented by the first EOF mode of the low-pass filtered summer (MJJAS) seasonal mean ω (Fig. 3), demonstrate intensification of convection in the oceanic TCZ and its weakening over the continental TCZ and therefore reflect a north–south dipole of convection. This mode explains 45.3% of the low-pass filtered seasonal mean ω.

The first SVD mode explains 86.2% of the total covariance between the low-pass filtered ISO-2 intensity and SST fields. This mode explains 29.3% of the ISO-2 variance. The SVD-1 spatial pattern for the ISO-2 intensity (Fig. 2c) is characterized by the three major action centers. Two centers over the eastern Indian Ocean and over the South China Sea demonstrate coherent changes in the ISO-2 intensity. We note that in these regions ISO-2 is the most pronounced (Fig. 1g). Opposite changes in the ISO-2 intensity are evident in the third action center over the Maritime continent. Together with its expansion coefficients (Fig. 2i)

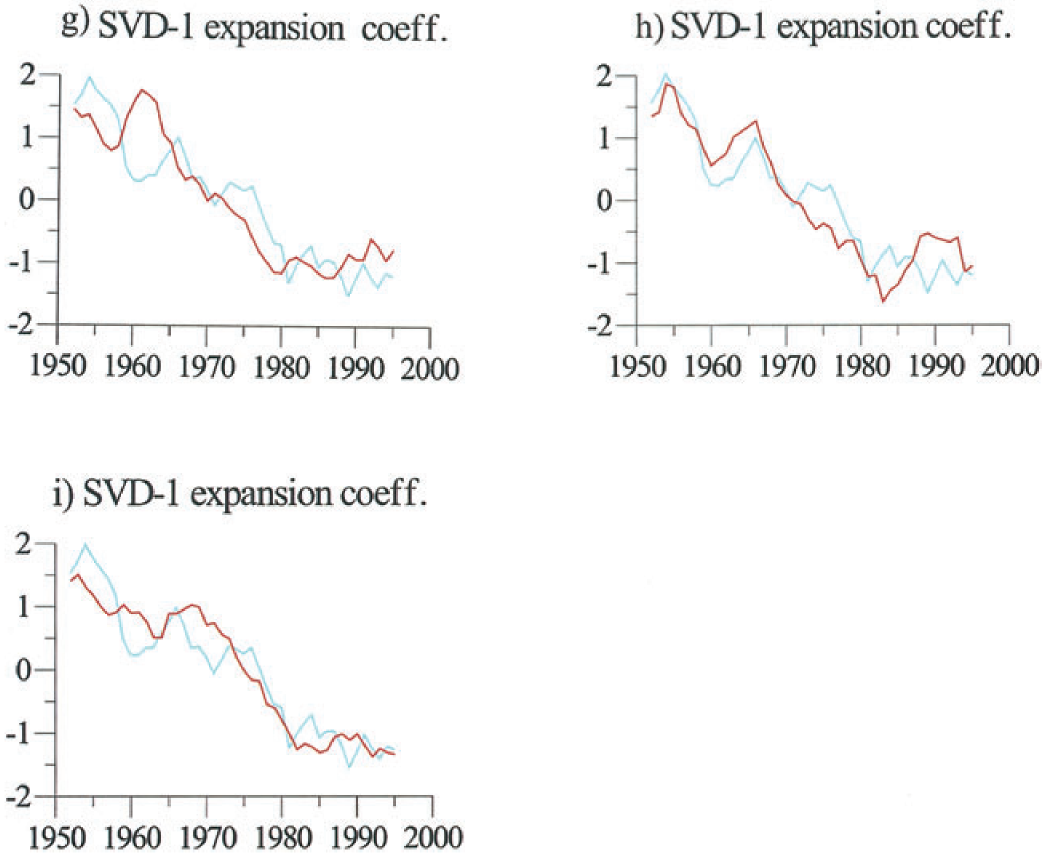

Fig. 2. The SVD-1 mode spatial patterns and expansion coefficients obtained for pairs of low-pass filtered U850-SST (a, d, g), ISO-1-SST (b, e, h), and ISO-2-SST (c, f, i). Expansion coefficients are normalized by their standard deviations. Red curve denotes U850, ISO-1 and ISO-2 variations. Blue curve reflects changes in SST.

this pattern shows an increase of the ISO-2 intensity over the eastern Indian Ocean and the South China Sea and a decrease over the Maritime continent during the considered time period. Again, the SVD-1 spatial pattern for SST (Fig. 2f) is very similar to those presented in Figs. 2d and e, and its description is omitted here. As in the two cases considered above (Figs. 2g and h), a climate regime shift in the mid-late 1970s is the major feature of temporal behaviour of the expansion coefficients of both the ISO-2 intensity and SST patterns (Fig. 2i). We note that in response to increased SST, ISO-2 has intensified in the regions of its climatological maxima (Fig. 1g) over the eastern Indian Ocean, the South China Sea and the western tropical Pacific, whereas the ISO-2 intensity has decreased in those regions where its activity is low (i.e. the Maritime continent, and in part the western Indian ocean).

5. Concluding remarks

In the present study we analyzed the variability in the summer mean 850 hPa zonal wind and in the intensities of ISO-1 (30–60 d oscillations) and ISO-2 (10–20 d oscillations) in the Asian summer monsoon system. The decadal–interdecadal variations contribute a considerable amount of variance to the total year-to-year variability for all of three parameters (i.e. mean zonal wind, intensities of ISO-1 and ISO-2). The decadal–interdecadal variations in the summer mean zonal wind and the ISO-1 intensity are the most pronounced in

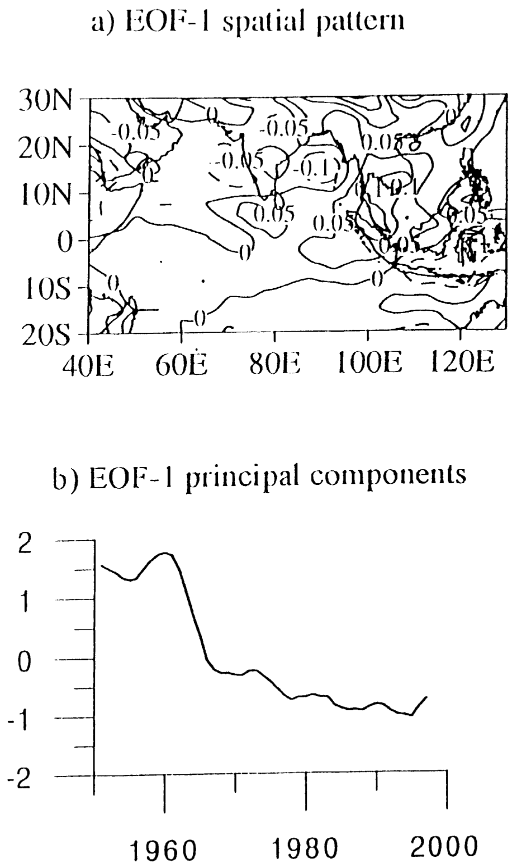

Fig. 3. Spatial pattern (a) and principal components (b) of the EOF-1 of low-pass filtered vertical velocity (ω) at 500 hPa level. Principal components are normalized by their standard deviations.

the band of strong westerlies extending from the Arabian Sea to the South China Sea and in the easterly flow south of the equator. The most prominent variations in the ISO-2 intensity on decadal–interdecadal time scales are found over the eastern Indian Ocean, the South China Sea and the western tropical Pacific.

The SVD analysis has shown that changes in the summer mean 850 hPa zonal wind and in the intensities of ISO-1 and ISO-2 are closely linked to interdecadal variations in the Indian Ocean SST. The major feature of temporal behaviour of SVD-1 expansion coefficients is the regime shift from positive to negative anomalies in the mid-late 1970s. The timing of this shift, which reflects interdecadal changes in the monsoon system, is the same as that of the North Pacific climate shift. Basically, SVD-1 patterns (and their expansion coefficients) of the SST represent local manifestation of the earlier detected interdecadal mode of SST variability with the strongest action center in the North Pacific extratropics (Zhang et al., 1997; Mantua et al., 1997). The temporal behaviour of this mode is characterized by the North Pacific climate regime shift in the mide-late 1970s, when SST in the central North Pacific sharply decreased, whereas SST in the tropical Indian and Pacific oceans increased (Nitta and Yamada, 1989; Tanimoto et al., 1993; Graham, 1994). The first SVD mode demonstrates weakening of the westerly flow on the interdecadal timescale over the northern Indian Ocean, Indian subcontinent, and Indochina. This is consistent with results of Sperber et al. (2000), who detected decrease of rainfall in the vicinity of India on the interdecadal timescale owing to weaker land–sea heat contrast, weaker dynamical monsoon index (Webster and Yang, 1992), and weaker westerlies.

Major features of the SVD-1 pattern for the ISO-1 intensity are its decrease over the northern Arabian Sea, Indian subcontinent, and the northern Bay of Bengal, and ISO-1 intensification south of this region over the Indian Ocean and the South China Sea. Important to note is that ISO-1 has intensified in the region of oceanic TCZ in response to SST increase (specifically strong in the equatorial central and western Indian Ocean) and more intensive convection (as shown by the EOF-1 mode of ω). Interdecadal warming in the Indian Ocean SST also resulted in intensification of ISO-2 activity over the eastern Indian Ocean, the South China Sea, and the western tropical Pacific. We note that in our preliminary EOF analysis of unfiltered data, which is not included in this study, we also found the first mode describing interdecadal changes and explaining 21–25% of the total variance of the summer mean 850 hPa zonal wind and the ISO intensities. Therefore, SVD analysis of low-pass filtered data allowed us to highlight these changes and to investigate links to SST variations on this particular timescale.

Our results obtained by the different method of analysis, in general, support and complement results of previous studies (Annamalai et al., 1999; Sperber et al., 2000), which suggested links between ISO activity and SST variations on decadal–interdecadal timescales. Moreover, our results show that not only the 30–60 d ISO mode, but also the 10–20 d ISO mode varies on interdecadal timescale.

6. Acknowledgements

The author thanks Diane Henderson and Dr. Gisela Speidel for their reading and careful editing of the manuscript. Discussions with Dr. H. Annamalai and his useful comments are greatly appreciated. Comments of Dr. K. Sperber and criticism of anonymous reviewers helped to improve the paper. Funding from the Frontier Research System for Global Change is greatly appreciated. This work was supported in part by the Russian Foundation for Basic Research (grant 98-05-64828). This paper is SOEST contribution number 5353, IPRC contribution number 128.

REFERENCES

Annamalai, H. and Slingo, J. M. 2001. Active/break cycles: diagnosis of the intraseasonal variability of the Asian summer monsoon. *Clim. Dynam.* **18**, 85–102.

Annamalai, H., Slingo, J. M., Sperber, K. N. and Hodges, K. 19991 The mean evolution and variability of the Asian summer monsoon: comparison of ECMWF and NCEP/NCAR Reanalyses. *Mon. Wea. Rev.* **127**, 1157–1186.

Bretherton, C. S., Smith, C. and Wallace, J. M. 1992. An intercomparison of methods for finding coupled patterns in climate data. *J. Clim.* **5**, 541–560.

Chen, T.-C. and Weng, S.-P. 1999. Interannual and intraseasonal variations in monsoon depressions and their westward-propagating predecessors. *J. Clim.* **12**, 1005–1020.

Duchon, C. E. 1979. Lanczos filtering in one and two dimensions. *J. Appl. Meteorol.* **18**, 1016–1022.

Ferranti, L., Slingo, J. M., Palmer, T. N. and Hoskins, B. J. 1997. Relations between interannual and intraseasonal monsoon variability as diagnosed from AMIP integrations, *Q. J. R. Meteorol. Soc.* **123**, 1323–1357.

Gadgil, S. and Asha, G. Intraseasonal variations of the Indian summer monsoon. Part I: Observational aspects. *J. Meteorol. Soc. Jpn.* **70**, 517–527.

Goswami, B. N. 1994. Dynamical predictability of seasonal monsoon rainfall: problems and prospects. *Proc. Ind. Natl. Sci. Acad.* **60A**, 101–120.

Goswami, B. N. and Mohan, R. S. A. 2001. Intraseasonal oscillations and interannual variability of the Indian summer monsoon. *J. Clim.* **14**, 1180–1198.

Graham, N. E. 1994. Decadal-scale climate variability in the tropical and North Pacific during the 1970s and 1980s: observations and model results. *Clim. Dynam.* **10**, 135–162.

Hartmann, D. L. and Michelsen, M. L. 1989. Intraseasonal periodicities in Indian rainfall. *J. Atmos. Sci.* **46**, 2838–2862.

Ju, J. and Slingo, J. M. 1995. The Asian summer monsoon and ENSO. *Q. J. R. Meteorol. Soc.* **122**, 1133–1168.

Kalnay, E., Kanamitsu, M., Kistler, R., Collins, W., Deaven, D., Gandin, L., Iredell, M., Saha, S., White, G., Wollen, J., Zhu, Y., Chelliah, M., Ebisuzaki, W., Higgins, W., Janowiak, J., Mo, K. C., Ropelewski, C., Wang, J., Leetma, A., Reynolds, R., Jenne, R. and Joseph, D. 1996. The NCEP/NCAR 40-year reanalysis project. *Bull. Am. Meteorol. Soc.* **77**, 437–471.

Kang, I.-S., Ho, C.-H., Lim, Y.-K. and Lau, K.-M. 1999. Principal modes of climatological seasonal and intraseasonal variations of the Asian summer monsoon. *Mon. Wea. Rev.* **127**, 322–340.

Krishnamurti, T. N. and Bhalme, H. N. 1976. Oscillations of the monsoon system. Part 1: Observational aspects. *J. Atmos. Sci.* **33**, 1937–1954.

Krishnamurthy, V. and Shukla, J. 2000. Intraseasonal and interannual variability of rainfall over India. *J. Clim.* **13**, 4366–4377.

Lanczos, C. 1956. *Applied analysis*. Prentice Hall, Englewood Cliffs, NJ, 539 pp.

Lau, K.-M. and Chan, P. H. 1988. Intraseasonal and interannual variations of tropical convection: a possible link between the 40–50 day oscillation and ENSO? *J. Atmos. Sci.* **45**, 506–521.

Madden, R. A. and Julian, P. R. 1971. Detection of a 40–50 day oscillation in the zonal wind in the tropical Pacific. *J. Atmos. Sci.* **28**, 702–708.

Madden, R. A. and Julian, P. R. 1972. Description of global scale circulation cells in the tropics with a 40–50 day period. *J. Atmos. Sci.* **29**, 1109–1123.

Mantua, N. J., Hare, S. R., Zhang, Y., Wallace, J. M. and Francis, R. 1997. A Pacific interdecadal climate oscillation with impacts on salmon production. *Bull. Am. Meteorol. Soc.* **78**, 1069–1079.

Mehta, V. M. and Lau, K.-M. 1997. Influence of solar irradiance on the Indian monsoon — ENSO relationship at decadal–multidecadal time scales. *Geophys. Res. Lett.* **24**, 159–162.

Nitta, T. and Yamada, S. 1989. Recent warming of tropical sea surface temperature and its relationship to the Northern Hemisphere circulation. *J. Meteorol. Soc. Jpn.* **67**, 375–382.

Parthasarathy, B., Munot, A. A. and Kothawale, D. R. 1994. All-India monthly and summer rainfall indices: 1871–1993. *Theor. Appl. Climatol.* **49,** 219–224.

Rao, R. R., Molinari, R. L. and Festa, J. F. 1989. Evolution of the climatological near-surface thermal structure of the tropical Indian Ocean. Part I: Description of mean monthly mixed layer depth, and sea surface temperature, surface current, and surface meteorological fields. *J. Geophys. Res.* **94**, 10,801–10,815.

Reynolds, R. W. and Smith, T. M. 1994. Improved global sea surface temperature analysis using optimum interpolation. *J. Clim.* **7**, 929–948.

Shukla, J. 1995. Predictability of the tropical atmosphere, the tropical oceans and TOGA. In *Proceedings of the International Conference on the Tropical Ocean Global Atmosphere (TOGA) Programme*, Vol. 2, WCRP-91, World Climate Research Programme, Geneva, Switzerland, 725–730.

Sikka, D. R. and Gadgil, S. 1980. On the maximum cloud zone and the ITCZ over Indian longitudes during the southwest monsoon. *Mon. Wea. Rev.* **108**, 1840–18536.

Slingo, J. M., Rowell, D. P., Sperber, K. R. and Nortley, F. 1999. On the predictability of the interannual behaviour of the Madden–Julian Oscillation and its relationship with El Niño. *Q. J. R. Meteorol. Soc.* **125**, 583–609.

Smith, T. M., Reynolds, R. W., Livezey, R. E. and Stokes, D. C. 1996. Reconstruction of historical sea surface temperatures using empirical orthogonal functions. *J. Clim.* **9**, 1403–1420.

Sperber, K. R., Slingo, J. M. and Annamalai, H. 2000. Predictability and the relationship between subseasonal and interannual variability during the Asian summer monsoon. *Q. J. R. Meteorol. Soc.* **126**, 2545–2574.

Tanimoto, Y., Iwasaka, N., Hanawa, K. and Toba, Y. 1993. Characteristic variations of sea surface temperature with multiple time scales in the North Pacific. *J. Clim.* **6**, 1153–1160.

Torrence, C. and Webster, P. J. 1999. Interdecadal changes in the ENSO-monsoon system. *J. Clim.* **12**, 2679–2690.

Vernekar, A. D. and Ji, Y. 1999. Simulation of the onset and intraseasonal variability of two contrasting summer monsoons. *J. Clim.* **12**, 1707–1725.

von Storch, H. and Navarra, A. 1995. *Analysis of climate variability*. Springer-Verlag, New York, 334.

Waliser, D. E., Zhang, Z., Lau, K. M. and Kim, J.-H. 2001. Interannual sea surface temperature variability and the predictability of tropical intraseasonal variability. *J. Atmos. Sci.* **58**, 2596–2615.

Wang, B. and Xu, X. 1997. Northern Hemisphere summer monsoon singularities and climatological intraseasonal oscillation. *J. Clim.* **10**, 1071–1085.

Webster, P. J. and Yang, S. 1992. Monsoon and ENSO: selectively interactive systems. *Q. J. R. Meteorol. Soc.* **118**, 877–926.

Webster, P. J., Magana, V. O., Palmer, T. N., Shukla, J., Tomas, R. A., Yanai, M. and Yasunari, T. 1998. Monsoons: processes, predictability, and the prospects for prediction. *J. Geophys. Res.* **103**, 14,451–14,510.

Weng, H., Lau, K.-M. and Xue, U. 1999. Multi-scale summer rainfall variability over China and its long-term link to global sea surface temperature variability. *J. Meteorol. Soc. Jpn.* **77**, 845–857.

Wilks, D. S. 1995. *Statistical methods in the atmospheric sciences*. Academic Press, Neew York, 467 pp.

Zhang, Y., Wallace, J. M. and Battisti, D. S. 1997. ENSO-like decadal variability over the Pacific sector. *J. Clim.* **10**, 1004–1020.